Electronic Supplementary Material (ESI) for Journal of Materials Chemistry C.

Supporting Information For: Multi-state emission properties and the inherent mechanism of D-A-D type asymmetric organic boron complexes

Yunpeng Qi, Yongtao Wang*, Guixian Ge*, Zhiyong Liu, Yongjiang Yu and Mei Xue

School of Chemistry and Chemical Engineering/Key Laboratory for Green Processing of Chemical Engineering of Xinjiang Bingtuan, Shihezi University, Shihezi 832003, Xinjiang, P. R. China. *E-mail: wyt_shzu@163.com; geguixian@126.com; Fax: +86 993 2057270; Tel: +86 993 2057277.

Experimental

Measurement and characterization

^{1}H NMR spectra were obtained with a Varian inova-400-MHz instrument using tetramethylsilane (TMS) as the internal standard. ^{13}C NMR spectra were recorded on a Varian inova-100-MHz spectrometer by using $CDCl_3$ as the solvent in all cases. The UV-vis absorption spectra were obtained on a MaPada UV-3200PCS spectrophotometer. Fluorescent emission spectra were obtained on a Hitachi F-2500 fluorescence spectrophotometer. Fluorescent quantum yields of solids were obtained by FLs980 full-featured Steady/Transient Fluorescence Spectrometer (Edinburgh). Glass transition temperature and melting point was determined by DSC measurements carried out using DSC Q2000 (TA, America). ESI/MS spectra were obtained on a Waters GCT Premier. MALDI/HRMS were record on an UltrafleXtreme MALDI-TOF/TOF mass spectrometer (Bruker, Germany). Powder XRD measurements were conducted on D8 Advance (Bruker) with Cu Kα radiation in the range $10^o < 2\theta < 90^o$. Digital photographs were taken by Canon 550D (Canon, Japan) digital cameras. Fluorescence lifetimes were obtained on an Edinburgh Instrument FLSP920 fluorescence spectrophotometer. Fluorescence microscopy photos were obtained on OLYMPUS BX53. The theoretical calculation were calculated by density functional theory (DFT) in Gaussian 09 at the B3LYP/6-31G (d,p) level. Fluorescence quantum yields in solution, for **TPEDKBF$_2$-**derivatives in various solvent were calculated versus quinine sulphate in 0.1 M sulfuric acid solution (Φ_F= 0.55) as the standard using the following values: η(Hexane) = 1.375, η(Toluene) = 1.496, η(CH_2Cl_2)= 1.424, η(THF) =1.405 η(DMSO) = 1.478, and η(H_2O) = 1.333. Optically dilute solutions of **TPEDKBF$_2$-**derivatives and quinine sulphate standard were prepared in 10 mL volumetric flasks with absorbances < 0.05. Quantum yield measurements were performed with excitation at λ ex = 350 nm.

Materials and Synthesis.

THF, DMF and CH_2Cl_2 were dried according to standardized procedures previously described. All the other chemicals and reagents used in this study were of analytical grade without further purification. In general, all the intermediates and final compounds were purified by column chromatography on silica gel (200-300 mesh), and crystallization from analytical grade solvents. Reactions were monitored by using thin layer chromatography (TLC). The synthetic routes for **TPEDKBF$_2$Ca, TPEDKBF$_2$DBeA,** and **TPEDKBF$_2$DMeA** are shown in Scheme 1. Firstly, TPE was synthesized by using benzophenone as the reagent according to the reported procedures; then Friedel-Crafts acylation reaction occurred between TPE and acetyl chloride, to thus give compound Ac-TPE; The boron complexes were synthesized by Claisen condensation with methyl benzoate derivatives and NaH (60%) to generate the β-diketones intermediates, followed by boronation with

$BF_3{\cdot}OEt_2$ in CH_2Cl_2. The target molecules were characterized by ^1H NMR, ^{13}C NMR, and MALDI-TOF mass spectrometry.

4-(4-(dibenzylamino)phenyl)-2,2-difluoro-6-(4-(1,2,2-triphenylvinyl)phenyl)-2H-1,3,2-dioxaborinin-1-ium-2-uide (TPEDKBF$_2$DBeA)

methyl 4-(dibenzylamino)benzoate (500 mg, 1.5 mmol), acetyl-TPE (520 mg, 1.40 mmol) and NaH (60%, 120 mg, 3.0 mmol) were added sequentially to a 100 mL round-bottom flask containing THF (30 mL). The mixture was refluxed under 90 ℃ for 24 h in argon atmosphere, it was cooled to room temperature. After that, the mixture was acidified with dilute HCl. The mixture was poured into water and extracted with dichloromethane three times. Then the organic phase was combined and dried over anhydrous Na_2SO_4. Removing the solvent under reduced pressure and an orange residue solid was collected. The residue was purified by column chromatography on silica gel eluting with petroleum ether/CH_2Cl_2, v/v = 3/1) to give the diketone precursor, 1-(4-(dibenzylamino)phenyl)-3-(4-(1,2,2-triphenylvinyl)phenyl)propane-1,3-dione as a yellow solid (500 mg, 53%) Then, the pure diketone precursor was dried under vacuum followed by dissolving in CH_2Cl_2 (50 mL). The boron trifluoride diethyl ether complex (0.3 mL, 2.4 mmol) was added to the above solution, which was stirred under an atmosphere of argon at room temperature for 24 h. Water was added in order to quench the reaction. The organic layer was separated and dried over Na_2SO_4. After removal of the solvent, the crude product was purified by column chromatography (silica gel, petroleum ether/CH_2Cl_2, v/v = 2/1) to afford **TPEDKBF$_2$DBeA** (428.5 mg) as a red solid, yield 80%, m.p. 190.0–192.0 °C. ^{1}HNMR (400 MHz, $CDCl_3$) δ/ppm = 7.98 (d,*J*=8.0, 2H), 7.80 (d,*J*=8.0, 2H), 7.39-7.29 (m, 6H)， 7.21 (d,*J*=8.0, 4H)，7.16-7.12 (m, 11H)， 7.04-7.00 (m, 6H)，6.88 (S, 1H), 6.81 (d,J=9.2, 2H), 4.78 (S, 4H), ^{13}C NMR (100 MHz, $CDCl_3$): δ/ppm = 180.63, 178.10, 154.84, 150.18, 143.18, 143.11, 143.02, 142.89, 139.73, 136.26, 131.99, 131.86, 131.35, 131.32, 131.28, 130.57, 129.06, 128.01, 127.95, 127.75, 127.68, 127.16, 126.90, 126.39, 119.44, 112.14, 91.61, 54.19. HRMS (MALDI-TOF): m/z 721.2951, calculated 721.2964.

4-(4-(dimethylamino)phenyl)-2,2-difluoro-6-(4-(1,2,2-triphenylvinyl)phenyl)-2H-1,3,2-dioxaborinin-1-ium-2-uide (TPEDKBF$_2$DMeA)

Compound **TPEDKBF$_2$DMeA** was prepared by following the synthetic procedure for compound **TPEDKBF$_2$DBeA**. The crude diketone precursor, 1-(4-(dimethylamino)phenyl)-3-(4-(1,2,2-triphenylvinyl)phenyl)propane-1,3-dione, was purified by column chromatography (silica gel, petroleum ether/CH_2Cl_2, v/v = 3/1), to afford pure diketone precursor (401 mg, 55%) as a yellow solid. Then, boronation with $BF_3{\cdot}OEt_2$ in CH_2Cl_2, the crude product was purified by column chromatography (silica gel, petroleum ether/CH_2Cl_2, v/v = 2/1) to obtain **TPEDKBF$_2$DMeA** (385 mg) as a red solid， yield 88%, m.p. 350.0–353.0 °C. ^{1}HNMR (400 MHz, $CDCl_3$) δ/ppm = 8.05 (d,*J*=8.0, 2H), 7.85 (d,*J*=8.4, 2H), 7.19-7.13 (m, 11H), 7.07-7.04 (m, 6H), 6.93 (s, 1H), 3.17 (s, 6H), ^{13}C NMR (100 MHz, $CDCl_3$): δ/ppm =155.09, 149.97, 143.12, 143.08, 143.04, 142.90, 139.75, 131.84, 131.82, 131.34, 131.31, 131.27, 127.98, 127.92, 127.72, 127.59, 126.87, 111.39, 99.98, 40.18. HRMS (MALDI-TOF): m/z 569.2334, calculated 569.2338.

4-(4-((9H-carbazol-9-yl))phenyl)-2,2-difluoro-6-(4-(1,2,2-triphenylvinyl)phenyl)-2H-1,3,2-dioxaborinin-1-ium-2-uide (TPEDKBF$_2$Ca)

Compound **TPEDKBF$_2$Ca** was prepared by following the synthetic procedure for compound **TPEDKBF$_2$DBeA**. The crude diketone precursor, 1-(4-(9H-carbazol-9-yl)phenyl)-3-(4-(1,2,2-triphenylvinyl)phenyl)propane-1,3-dione, was purified by column chromatography (silica gel, petroleum ether/CH_2Cl_2, v/v = 3/1), to afford pure diketone precursor (459 mg, 51%) as a yellow solid. Then, boronation with $BF_3{\cdot}OEt_2$ in CH_2Cl_2, the crude product was purified by column chromatography (silica gel, petroleum ether/CH_2Cl_2, v/v = 2/1) to obtain **TPEDKBF$_2$DCa** (420 mg) as a red solid, yield 85%, m.p. 268.0–270.0 °C. ^{1}HNMR (400 MHz, $CDCl_3$) δ/ppm = 8.39 (d,J=8.8, 2H), 8.17 (d,*J*=8.0, 2H), 7.96 (d,*J*=8.0), 7.85 (d,*J*=8.8, 2H), 7.56 (d,*J*=8.0, 2H), 7.48

(td,*J*=8.0, 2H), 7.37 (td,*J*=8.0), 7.26 (d,*J*=8.8, 2H), 7.20-7.15 (m, 10H), 7.09-7.04 (m, 6H), ^{13}C NMR (100 MHz, $CDCl_3$): δ/ppm = 182.62, 180.99, 152.08, 144.11, 143.95, 142.87, 142.66, 139.83, 139.46, 132.21, 131.35, 131.26, 130.62, 130.00, 129.57, 128.56, 128.11, 128.06, 127.79, 127.38, 127.07, 126.51, 126.42, 124.19, 121.15, 120.59, 109.84, 99.98, 93.33. HRMS (MALDI-TOF): m/z 672.2518, [[M-F]$^+$, calculated 672.2510].

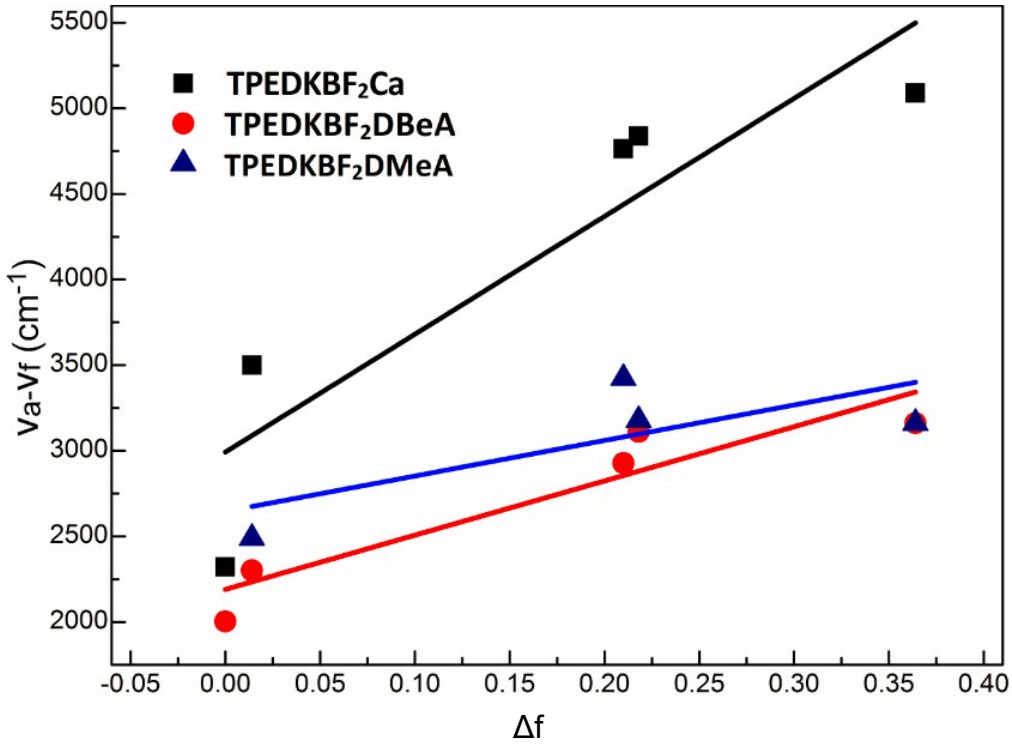

Figure S1. Lippert–Mataga plot of **TPEDKBF$_2$Ca**, **TPEDKBF$_2$DBeA** and **TPEDKBF$_2$DMeA** *vs* the solvent polarity.

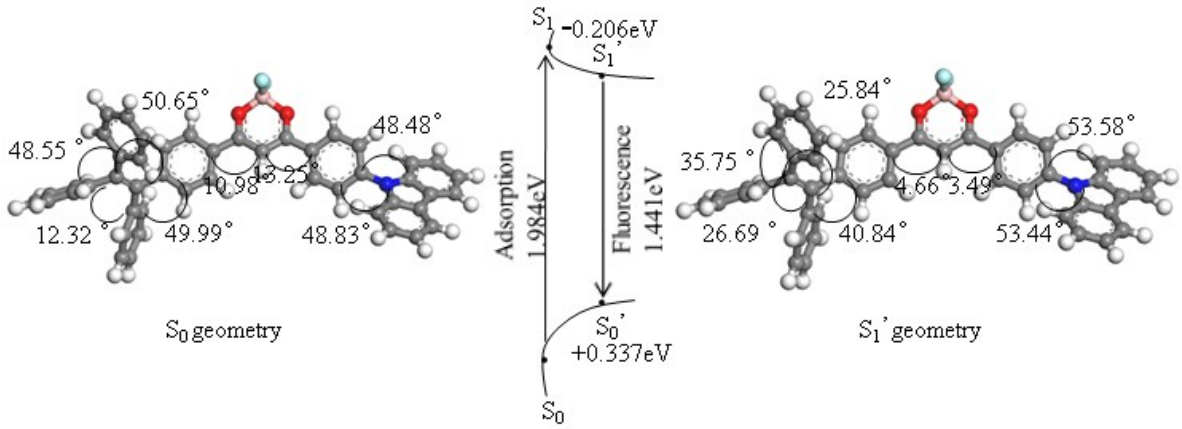

Figure S2. Optimized structures for the S_0 (S_0) and S_1 (S_1') electronic states and an energy diagram for **TPEDKBF$_2$Ca**, calculated at the B3LYP/SV(P) level of theory.

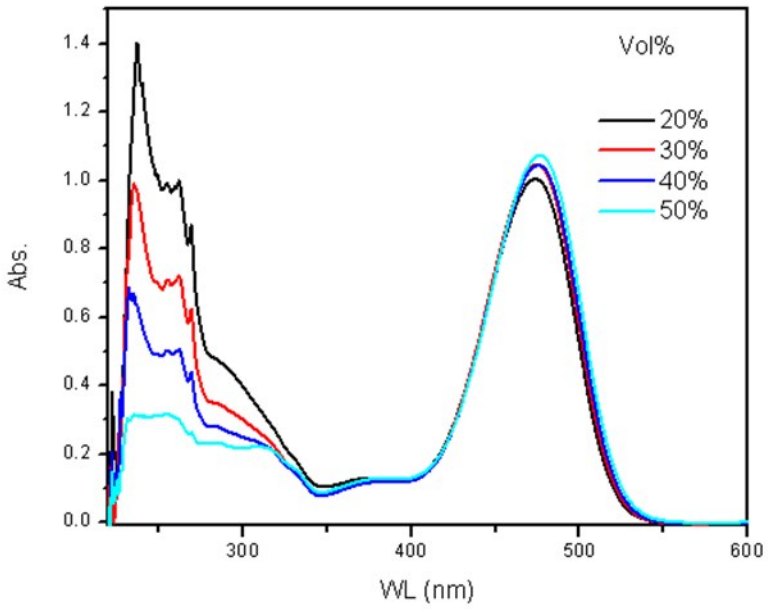

Figure S3. The UV-Vis absorption spectrum of TPEDKBF$_2$DBeA from 20 to 50% water content (4nm red-shift)

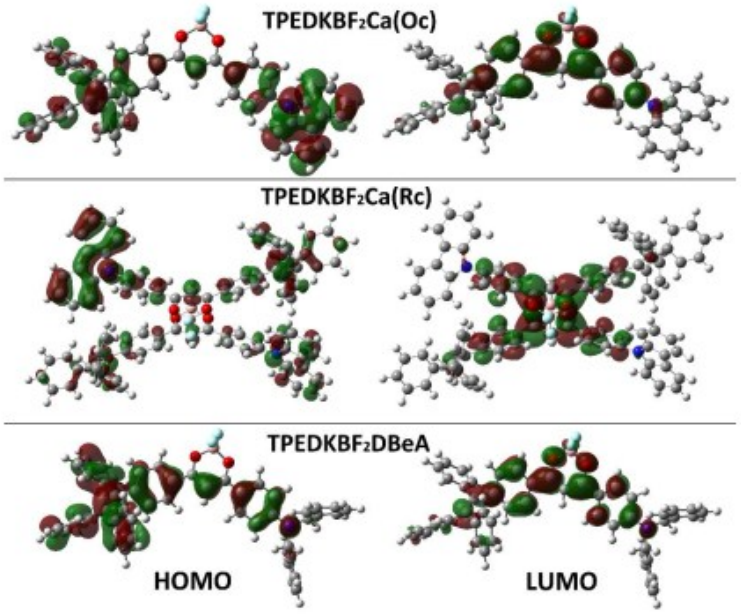

Figure S4. The frontier orbital plots of the HOMO and LUMO of molecular **TPEDKBF$_2$Ca**，**TPEDKBF$_2$DBeA**，**TPEDKBF$_2$DMeA** in single crystal.

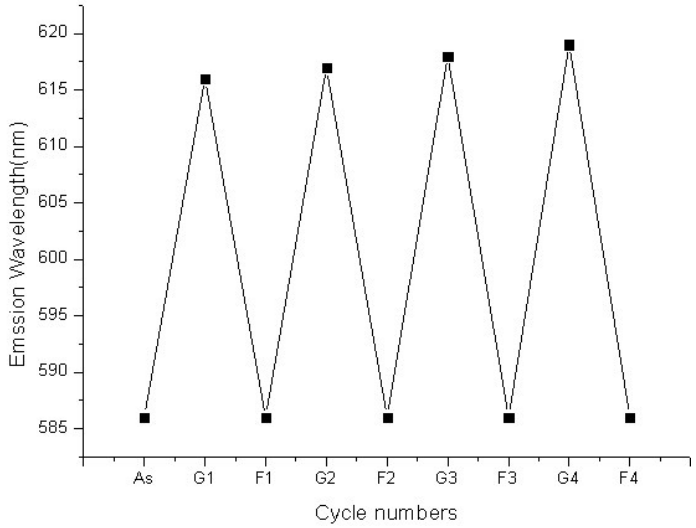

Figure S5. Emission maxima of TPEDKBF$_2$Ca（Oc） during the grinding-annealing cycles. As = the prepared crystals of TPEDKBF$_2$Ca (Oc), G = ground sample; Fn= Fuming sample (fuming with DCM for 2h). The numbers after G or Fn represent cycle numbers.

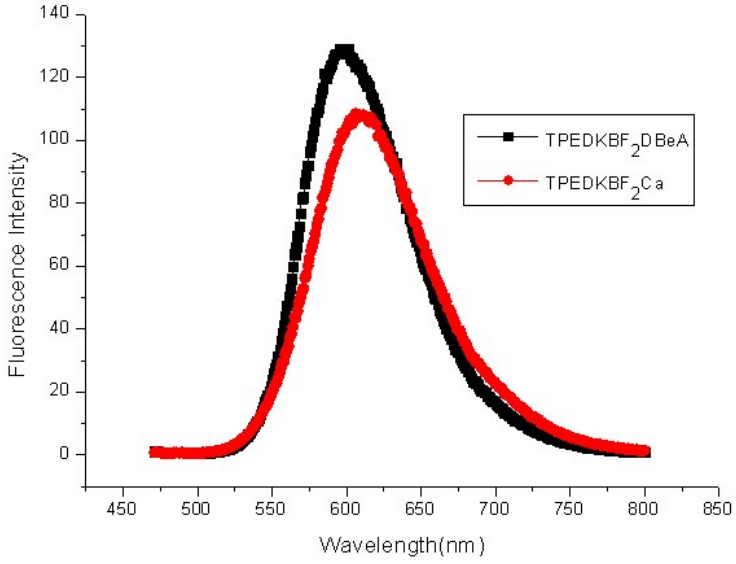

Figure S6. Fluorescent spectra of TPEDKBF$_2$DBeA(Φ_F=o.538)and TPEDKBF$_2$Ca(Φ_F =0.570)at the melt-cooled amorphous states

Table S1. Peak absorption/emission wavelengths (λ, in nm) and quantum yields (Φ_F) of three compounds in different solvents.

	Φ_F/%			λ_{abs}/ λ_{em}		
	TPEDKBF$_2$Ca	**TPEDKBF$_2$DBeA**	**TPEDKBF$_2$DMeA**	**TPEDKBF$_2$Ca**	**TPEDKBF$_2$DBeA**	**TPEDKBF$_2$DMeA**
Hexane	1.3	13.9	--	448/500	453/497	--
Toluene	1.7	23.1	45.5	457/544	465/522	469/531
DCM	0.5	7.4	11.4	459/590	474/556	479/565
THF	0.8	20.4	4.3	451/576	470/545	472/563
DMSO	--	3.0	0.2	462/606	488/577	492/585

Table S2. HOMO/LUMO energy levels of **TPEDKBF$_2$Ca**, **TPEDKBF$_2$DBeA**, **TPEDKBF$_2$DMeA.**

	single molecular state/single crystal		
	gap（eV）	LUMO（eV）	HOMO（eV）
TPEDKBF$_2$Ca(Oc)	2.908/2.915	-2.689/-2.691	-5.597/-5.606
TPEDKBF$_2$Ca(Rc)	2.908/2.694	-2.689/-2.792	-5.597/-5.486
TPEDKBF$_2$DBeA	3.181/3.182	-2.282/-2.294	-5.463/-5.476
TPEDKBF$_2$DMeA	3.189/ --	-2.255/ --	-5.445/ --

Table S3. Peak emission wavelengths (λ, in nm), fluorescent lifetime (τ, in μs) and quantum yields of five compounds in different states.

Entry	$\lambda_{ultrasonic}$	$\lambda_{crystal}$	[c] λ_{ground}	λ_{fumed}	$\lambda_{annealed}$	$\Delta\lambda_{max}$	$\Phi_{crystal}$	Φ_{ground}	$\tau_{crystal}$	τ_{ground}
TPEDKBF$_2$DBeA	617	642	597	603	600	45	0.188	0.545	8.503	8.143
TPEDKBF$_2$DMeA	624	628	636	630	628	12	0.157	0.211	0.268	0.073
TPEDKBF$_2$Ca(Oc)	581	586	616	582	583	35	0.550	0.566	3.839	4.515
TPEDKBF$_2$Ca(Rc)	582	624	615	583	583	9	0.485	--	--	--

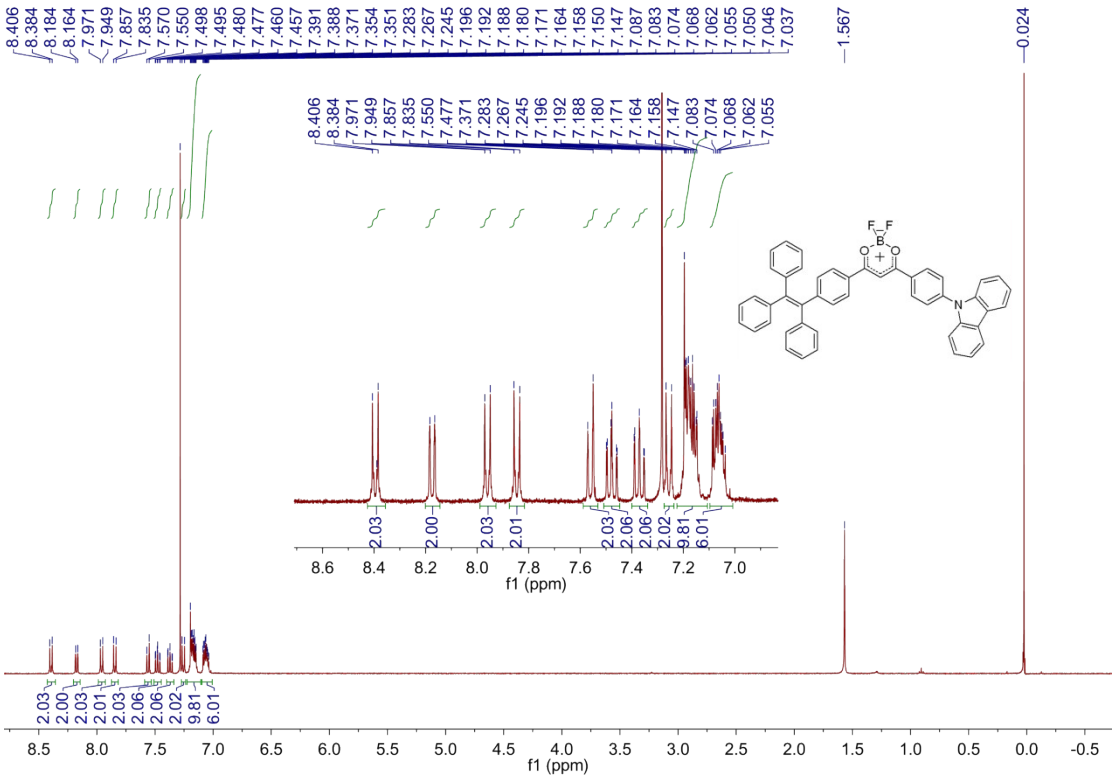

Figure S7 ^{1}H NMR (400 MHz) spectrum of compound **TPEDKBF$_2$Ca** in $CDCl_3$.

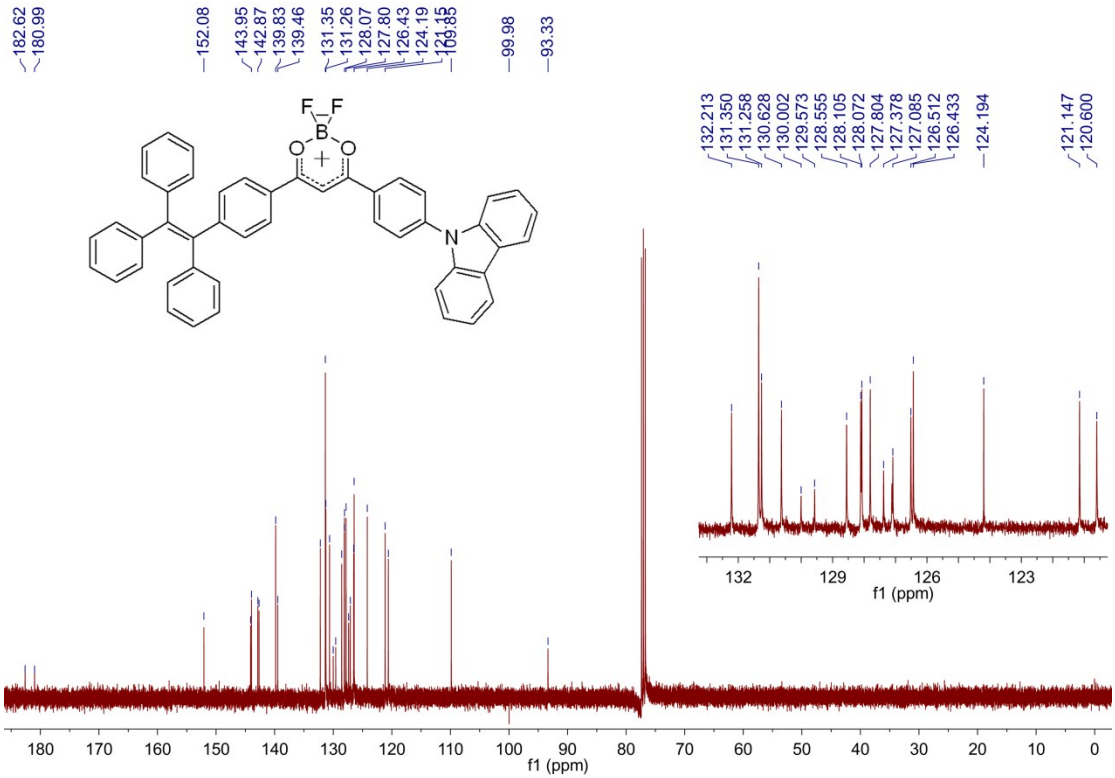

Figure S8 ^{13}C NMR (100 MHz) spectrum of compound **TPEDKBF$_2$Ca** in $CDCl_3$.

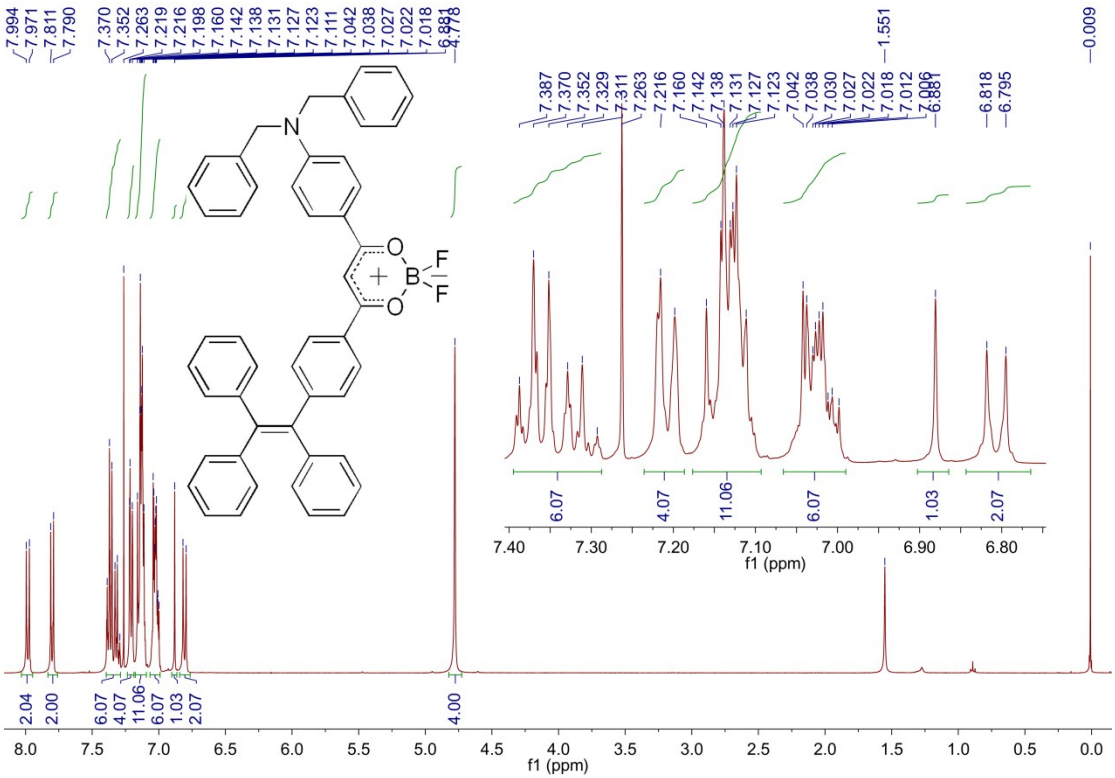

Figure S9 ^{1}H NMR (400 MHz) spectrum of compound **TPEDKBF$_2$DBeA** in $CDCl_3$.

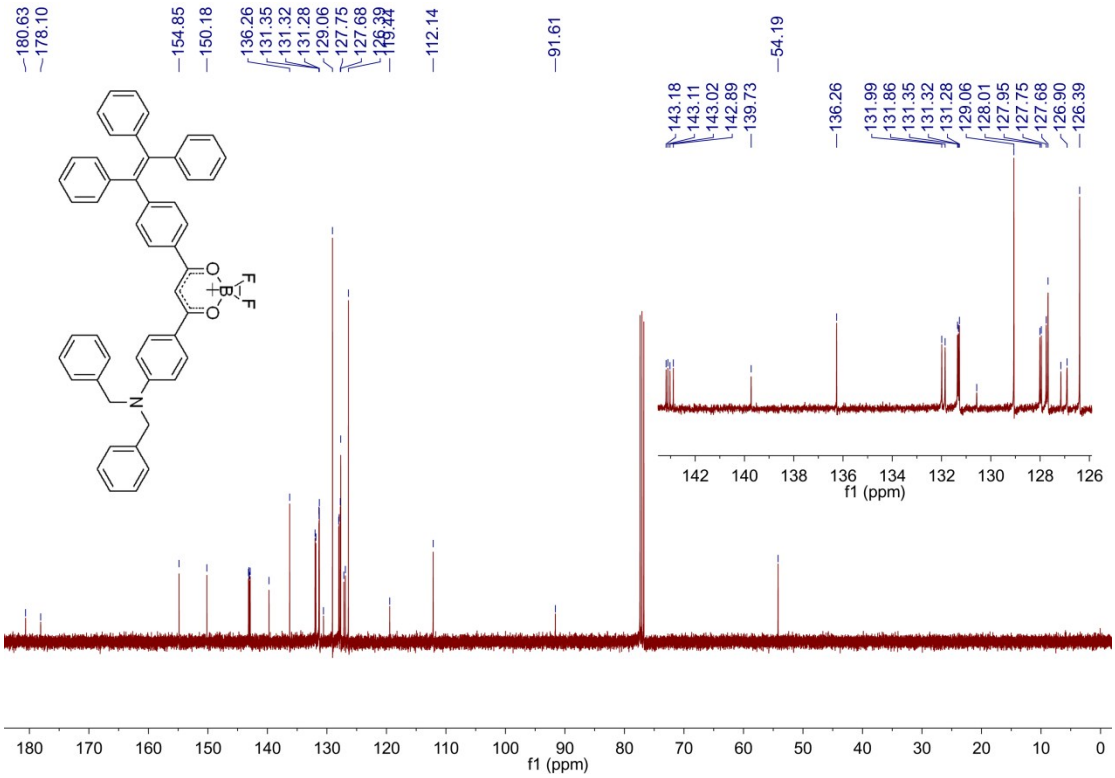

Figure S10 ^{13}C NMR (100 MHz) spectrum of compound **TPEDKBF$_2$DBeA** in $CDCl_3$.

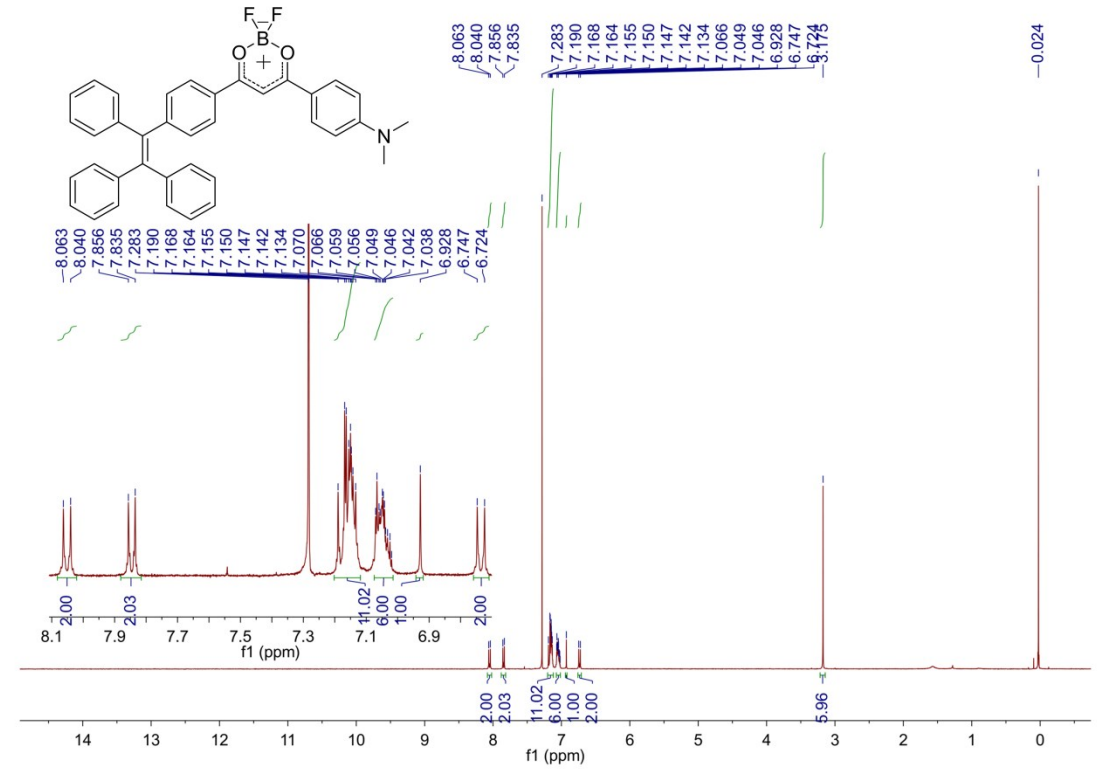

Figure S11 ^{1}H NMR (400 MHz) spectrum of compound **TPEDKBF$_2$DMeA** in $CDCl_3$.

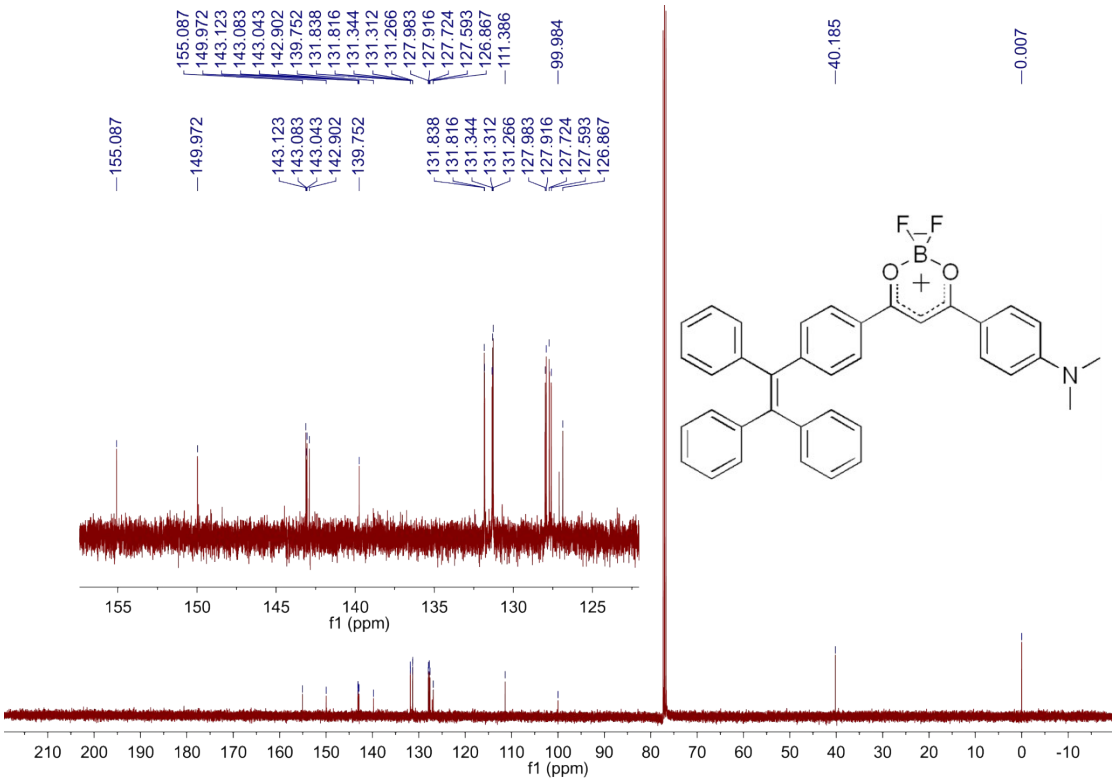

Figure S12 ^{13}C NMR (100 MHz) spectrum of compound **TPEDKBF$_2$DMeA** in $CDCl_3$.

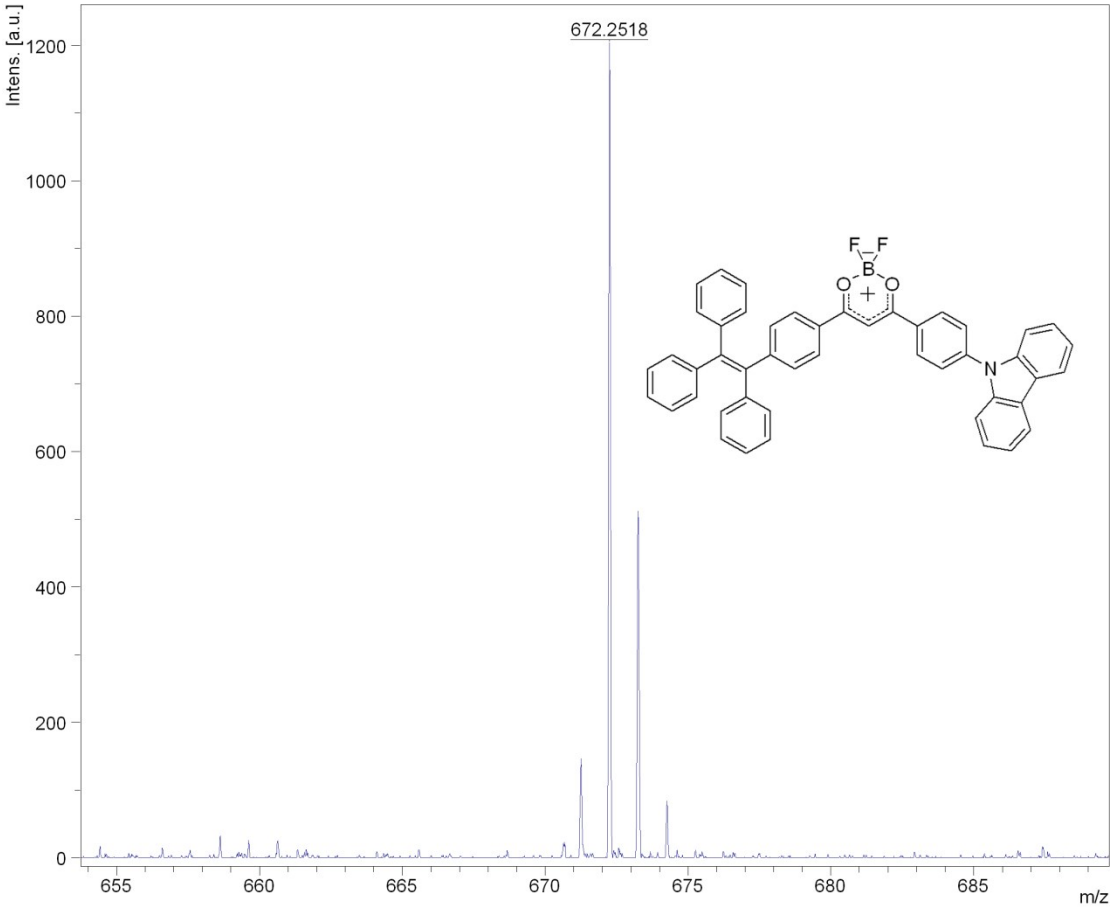

Figure S13 MALDI/TOF MS spectrum of compound **TPEDKBF$_2$Ca**.

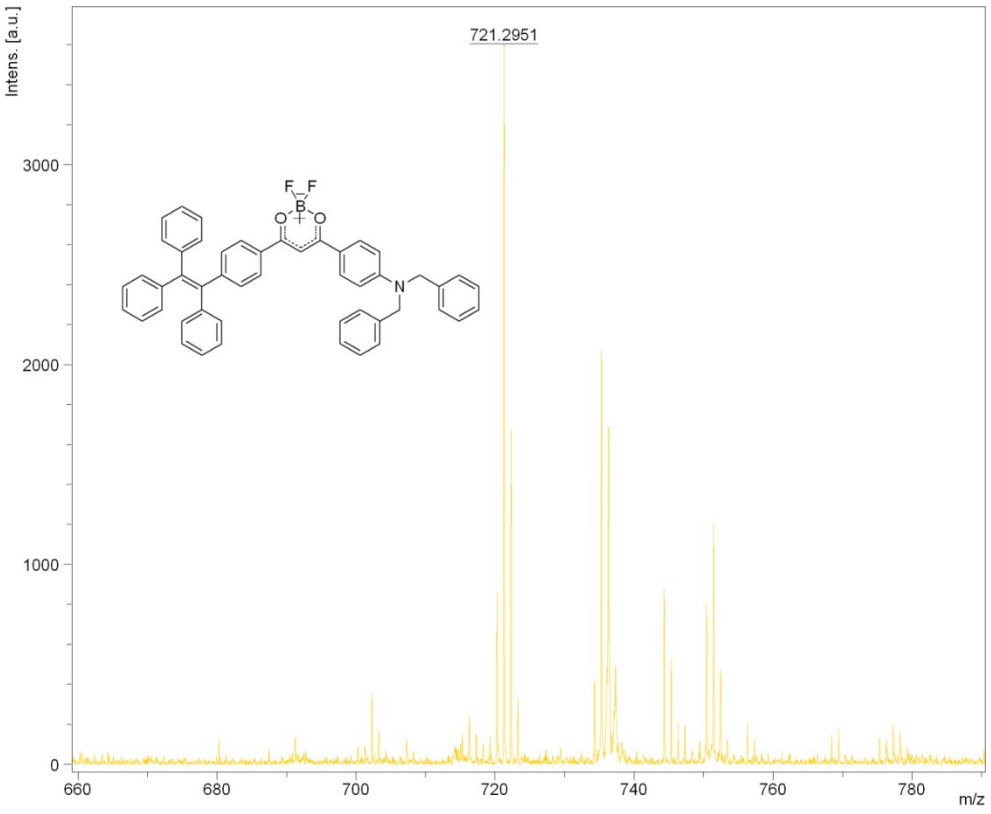

Figure S14 MALDI/TOF MS spectrum of compound **TPEDKBF$_2$DBeA**.

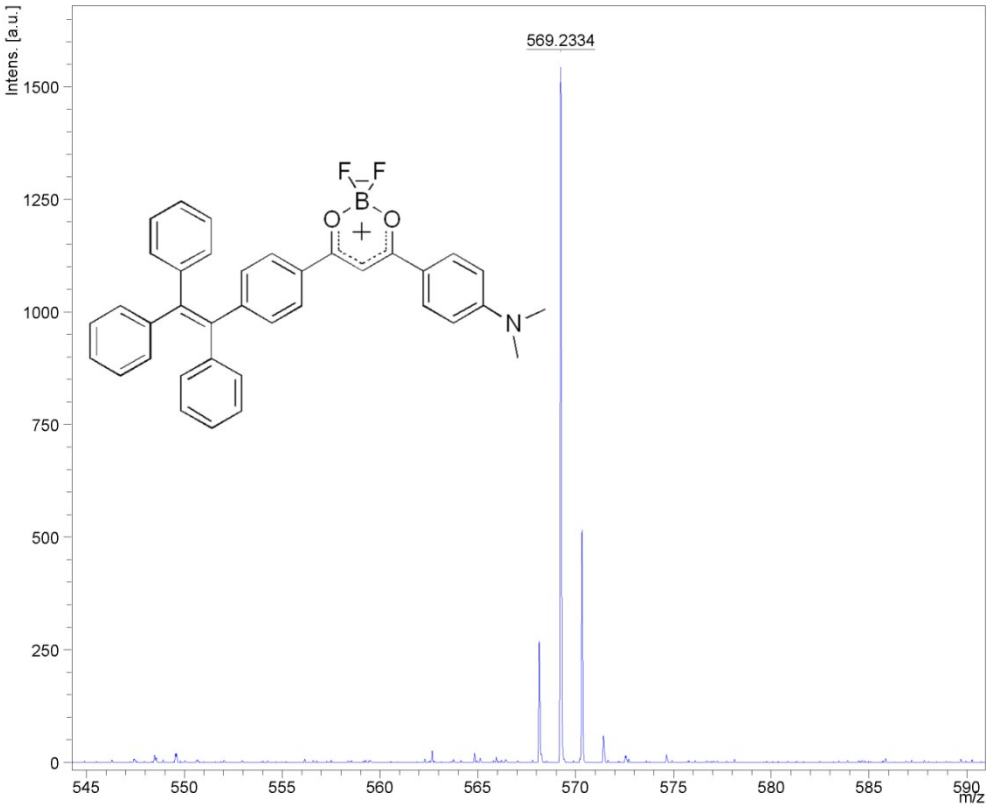

Figure S15 MALDI/TOF MS spectrum of compound **TPEDKBF$_2$DMeA**.

Table S4: Crystal data and structure refinement for the single crystals

	TPEDKBF$_2$Ca (Oc)	**TPEDKBF$_2$DBeA**	**TPEDKBF$_2$Ca (Rc)**
Empirical formula	C47 H32 B F2 N O2	C49 H38 B F2 N O2	C47 H32 B F2 N O2
Formula weight	691.55	721.61	691.55
Temperature, K	296(2)	296(2)	296(2)
Wavelength, Å	0.71073	0.71073	0.71073
Crystal system	Triclinic	Triclinic	Monoclinic
space group	P-1	P-1	P2(1)/n
a, Å	8.3426(9)	8.393(5)	14.917(2)
b, Å	11.4056(11)	11.122(7)	24.663(3)
c, Å	19.6777(18)	21.214(13)	20.762(3)
α, deg.	81.770(3)	97.698(17)	90.00
β, deg.	84.375(3)	96.901(15)	93.468(5)
γ, deg.	87.955(4)	91.598(18)	90.00
Volume, Å^3	1843.7(4)	1946(2)	7624.1(19)
Z	2	2	8
Calculated density	1.246 Mg/m^3	1.231 Mg/m^3	1.205 Mg/m^3
Absorption coefficient	0.082 mm^{-1}	0.080 mm^{-1}	0.079 mm^{-1}
F(000)	720	756	2880
Crystal size	0.21 x 0.17 x 0.19 mm	0.20 x 0.19 x 0.18 mm	0.22 x 0.20 x 0.18 mm
Theta range for data	1.05 to 24.96 deg.	0.98 to 25.11 deg.	1.28 to 25.00 deg.

collection			
Limiting indices	-9<=h<=8, -13<=k<=13, -23<=l<=23	-9<=h<=9, -9<=k<=13, -25<=l<=23	-15<=h<=17, -29<=k<=28, -24<=l<=24
Reflections collected / unique	11808/6382 [R(int)=0.0381]	12304/6820 [R(int)=0.0941]	14145/7034[R(int)=0.0293]
Completeness to theta	24.96˚, 98.6 %	25.11˚, 98.4 %	25.00˚, 99.9 %
Absorption correction	Semi-empirical from equivalents	Semi-empirical from equivalents	Semi-empirical from equivalents
Max. and min. transmission	0.9847 and 0.9816	0.9857 and 0.9841	0.9859 and 0.9828
Refinement method	Full-matrix least-squares on F^2	Full-matrix least-squares on F^2	Full-matrix least-squares on F^2
Data / restraints / parameters	6382 / 0 / 479	6820 / 0 / 496	13413 / 48 / 956
Goodness-of-fit on F^2	0.967	0.937	1.479
Final R indices [I>2sigma(I)]	R_1 = 0.0558, wR_2 = 0.1287	R_1 = 0.1140, wR_2 = 0.3079	R_1 = 0.1564, wR_2 = 0.4437
R indices (all data)	R_1 = 0.1148, wR_2 = 0.1613	R_1 = 0.2587, wR_2 = 0.3985	R_1 = 0.2517, wR_2 = 0.4936
Largest diff. peak and hole	0.238 and -0.262 e. $Å^{-3}$	0.283 and -0.338 e. $Å^{-3}$	2.797 and -0.460 e. $Å^{-3}$